Neutron scattering experiments on $YbXCu_4$ and $ErXCu_4$ (X = Au, Pd, and Ag)

A. Severing and A. P. Murani
Institut Laue-Langevin, Grenoble, France

J. D. Thompson and Z. Fisk
Los Alamos National Laboratory, Los Alamos, New Mexico 87545

C.-K. Loong
Argonne National Laboratory, Argonne, Illinois 60439

(Received 13 June 1989)

Temperature-dependent neutron scattering experiments with incident energies in the range 3–50 meV have been performed on polycrystalline samples of the heavy-electron system $YbXCu_4$, as well as the stable $4f$-moment compounds $ErXCu_4$ and the nonmagnetic reference materials $LuXCu_4$, with X = Au, Pd, and Ag. The quasielastic linewidth of the $YbXCu_4$ compounds is determined as a function of temperature. For $YbAuCu_4$ a quantitative crystal-field analysis is applied to the observed inelastic response, while the data for the strongly $4f$-delocalized compound $YbAgCu_4$ are discussed in terms of a possible crystal-field interpretation and various theoretical models for heavy-electron systems.

INTRODUCTION

At low temperatures the heavy-electron metallic compounds and alloys exhibit a rich variety of phenomena, ranging from localized moment formation through Kondo and intermediate-valence behavior to magnetic and superconducting ordering. Although the origin of these anomalous properties is not yet fully understood, they are related to hybridization of the $4f$ electrons with the conduction-band states and the associated many-electron dynamics in the proximity of the Fermi level. Among the heavy-electron materials rare-earth compounds containing Ce and Yb have been the subject of numerous investigations. Recently, a new series of heavy-fermion Yb compounds $YbXCu_4$ with X = Ag, Au, and Pd were reported by Rossel *et al.*[1] with effective electron masses as high as $\simeq 60m_e$ (where m_e is the mass of the free electron). Inelastic neutron scattering probes the energy and wave-vector-dependent dynamic susceptibility, which provides information concerning low-lying excitations above the ground state. Model calculations for heavy-electron systems predict that the f electronic levels described by a crystal-field potential will be strongly renormalized because of the highly correlated electron ground state. Therefore, it is of interest to examine to what extent the results of neutron experiments are consistent with models describing electronic correlations and/or crystal-field effects.

In this paper we present results of inelastic neutron scattering experiments on the isostructural compounds $YbXCu_4$ and $ErXCu_4$ with X=Au, Pd, and Ag. The Yb-based compounds show strong electronic correlations in specific heat, resistivity, and static susceptibility measurements.[1] Within the field of heavy-fermion, Kondo, or intermediate-valent materials, the $YbXCu_4$ compounds are ideally suited for comparison with theoretical models because of the cubic site symmetry of Yb ions in the $AuBe_5$ structure. Furthermore, the interaction between Yb magnetic moments should be weak because of the large Yb-Yb distances ($\simeq 5$ Å). The stable $4f$-moment Er compounds are measured as references to assist in determining of the influence of electronic correlations of Yb on the quasielastic and/or inelastic magnetic scattering response. We chose the Er series as the magnetic reference since Er^{3+}, in contrast to Tm^{3+}, has the advantage of being a Kramer's ion (half-integral total angular momentum) so that the crystal-field schemes are easier to determine. Furthermore, Er is preferable to other Kramer's ions such as Dy and Nd, since it is closer to Yb in the periodic table.

$YbAuCu_4$ and $YbPdCu_4$ appear to order antiferromagnetically at 0.6 and 0.8 K, respectively, whereas $YbAgCu_4$ does not show any sign of ordering down to 0.45 K.[1] The electrical resistivity ρ of all three Yb compounds shows only a small temperature dependence above 80 K. Below 60 K the resistivity of $YbAgCu_4$ falls rapidly and at $T<28$ K it follows a T^2 power law below 28 K, which is characteristic of Fermi-liquid behavior or spin fluctuations. The resistivity of the Au- and Pd-based Yb compounds exhibits Kondo-like behavior with a minimum located at about 85 K for X=Au and $\simeq 60$ K for X=Pd. At about 1 K, ρ of $YbAuCu_4$ and $YbPdCu_4$ displays a sharp maximum that is associated with the onset of magnetic order.[1] The magnetic susceptibility χ_{bulk} of $YbAuCu_4$ and $YbPdCu_4$ follows a Curie-Weiss law. For $T \le 30$ K the inverse susceptibility $1/\chi_{\text{bulk}}$ deviates only slightly from linearity. In contrast to the X=Au and Pd samples, $YbAgCu_4$ shows a susceptibility typical of materials with an unstable $4f$ shell (see Fig. 10): for $T>100$ K, χ_{bulk} exhibits Curie-Weiss behavior, then goes through a maximum at $T \simeq 35$ K and reaches a constant value for $T \to 0$. Specific-heat measurements of the $YbXCu_4$ compounds yield large linear coefficients γ of 245 mJ/mol K^2 for $YbAgCu_4$ and 200 mJ/mol K^2 for $YbPdCu_4$, in addition to the magentic ordering contribution at low T in the latter compound.[2] In a double logarithmic plot of γ versus χ_{bulk} the values for $YbAgCu_4$ fall within the cluster of other heavy-fermion compounds. For $YbPdCu_4$, however, the susceptibility appears to be too large with respect to γ (i.e., it deviates strongly from the linear $\gamma/\chi = 1$ relation).

The static susceptibility of the $ErXCu_4$ samples indicates ferromagnetic ordering transitions between $T=5$ and 10 K. This temperature range is in agreement with temperatures we obtain from de Gennes scaling from Yb^{3+} to Er^{3+} under the assumption that ordering and Curie-Weiss temperatures are comparable.

EXPERIMENTAL

The polycrystalline $YbXCu_4$ samples were prepared by melting the pure elements in a scaled Ta tube, whereas the magnetic reference compounds $ErXCu_4$ and the nonmagnetic reference compounds $LuXCu_4$ (X=Ag, Au, and Pd) were prepared by arc melting. Bulk susceptibility measurements were performed to verify that the magnetic properties of our samples are the same as reported in Ref. 1. Susceptibility measurements on the Er samples indicated ferromagnetic order as mentioned earlier. X-ray and neutron-diffraction measurements show that all samples crystallize in the $AuBe_5$ structure (space group $C15b$ or F-$43m$) and that they are single phased, except the Pd-based samples, which contain other impurity phases. The Bragg lines of $YbPdCu_4$, $ErPdCu_4$, and $LuPdCu_4$ are strongly broadened, which might be due to the presence of several disordered $R_{1-x}Pd_{1+x}Cu_4$ phases (R=Yb, Er, and Lu) with space group $C15$. In a disordered sample with space group $C15$ the cubic-site symmetry of the rare-earth ions is destroyed, with attendant consequences on the inelastic magnetic spectrum. The room-temperature lattice constants of the Yb samples agree with the ones given in Ref. 1 (a =7.0696, 7.0519, and 7.0396 Å for X =Ag, Au, and Pd). For $ErXCu_4$ we obtain a=7.098, 7.072, and 7.064 Å for X=Ag, Au, and Pd, respectively.

The double differential cross section for paramagnetic scattering as measured with unpolarized neutrons is given by

$$(|k_i|/|k_f|)d^2\sigma/d\Omega\, d\omega = NS(Q,\omega) = \frac{AN}{[1-\exp(-\hbar\omega/k_BT)]}\chi''(Q,\omega) ,$$

where N is the number of magnetic scatterers, k_i and k_f are the initial and final neutron wave vectors, $S(Q,\omega)$ is the scattering function, $A=\frac{1}{2}(g_N r_e/\mu_B)^2$ is the coupling between the neutron and electron spin, and $\chi''(Q,\omega)$ is the imaginary part of the dynamic susceptibility. From the Kramers-Kronig relation $\chi''(Q,\omega)$ can be expressed in terms of the static susceptibility $\chi(Q)$ and a spectral function $P(Q,\omega)$

$$\chi''(Q,\omega) = \pi\omega\chi(Q)P(Q,\omega) .$$

The static susceptibility $\chi(Q)$ is related to the static bulk susceptibility χ_{bulk} (susceptometer value) via the local magnetic form factor $F(Q)$, $\chi(Q) = |F(Q)|^2\chi_{bulk}$. $P(Q,\omega)$ is a spectral function which, in accordance with the Kramers-Kronig relation, must fulfill the normalization condition $\int_{-\infty}^{\infty} P(Q,\omega)d\omega = 1$. When describing relaxation processes $P(Q,\omega)$ is usually assumed to be Lorentzian. In the presence of crystal-field splittings $P(Q,\omega)$ is described by a series of Lorentzians centered at $\hbar\omega=0$ (quasielastic) and $\pm\hbar\omega_i$ (crystal-field excitations). However, in compounds with strong $4f$-conduction electron scattering $P(Q,\omega)$ shows deviations from a quasielastic Lorentzian line shape as reported previously[3-8] and as discussed later.

The neutron measurements were performed on three different time-of-flight (TOF) spectrometers, each best adapted for a different incident energy, thus permitting an investigation of the quasielastic as well as the inelastic parts of the spectra. The instruments are located at the Intense Pulsed Neutron Source (IPNS) at Argonne National Laboratory, and at the High-Flux Reactor at the Institut Laue-Langevin (ILL) in Grenoble, France. In Table I we list the instruments, their location, the respective incident energies E_0 and energy resolutions ΔE [full width at half maximum (FWHM) at elastic position] and the lowest available temperatures during the experiment.

At each of the instruments, the background scattering was determined by measurements with the empty sample holder and a cadmium plate in the sample position. All spectra shown are treated with the same data correction and fitting routines that include energy- and angle-dependent absorption as well as detector efficiency corrections. The data are calibrated for absolute units of cross section with reference to a vanadium standard. Furthermore, for IN6 the rapid change of the resolution function with energy transfer due to the time focusing is taken into account in the data treatment. The statistical error in the spectra is reflected by the scatter in the data points. For the phonon correction the nonmagnetic reference compounds $LuXCu_4$ (X=Ag, Au, and Pd) were measured. In Fig. 1 a $LuAuCu_4$ and a $LuAgCu_4$ spectrum are shown for incident energies of E_0=40 meV and E_0=3.14 meV, respectively. Since the phonon scattering is rather weak in comparison to the magnetic scattering,

TABLE I. E_0 incident energy, ΔE energy resolution at elastic position, and T lowest reachable temperature for the time-of-flight (TOF) spectrometers employed.

TOF Instrument	Location	E_0 (meV)	ΔE (meV) FWHM	T (K)
HRMECS	IPNS	40	1.2	>15
IN4[a]	ILL	50	2.8	>5
IN4[b]	ILL	17	0.75	>5
IN4[a]	ILL	12.5	0.65	>5
IN6	ILL	3.14	0.09	>1.5

[a]Double graphite monochromator version.
[b]Single graphite monochromator version.

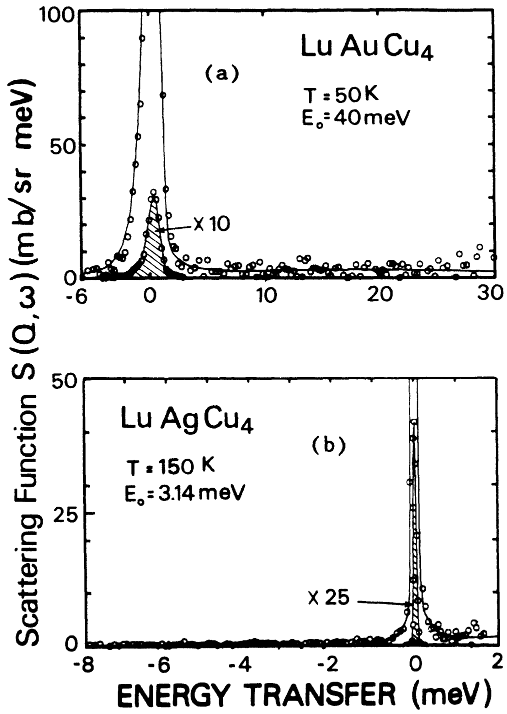

FIG. 1. Spectra of nonmagnetic reference compounds: (a) energy-loss side (of the neutron) of the $LuAuCu_4$-spectrum (HRMECS), scattering angle θ within $-7^\circ \leq 2\theta \leq 19^\circ$; (b) energy-gain side of the $LuAgCu_4$ spectrum (IN6), $17^\circ \leq 2\theta \leq 34^\circ$.

it does not show much structure at either energies, and the phonon corrections were performed by simply subtracting the observed intensities for the Lu-based samples allowing for the different scattering lengths of Yb and Lu. The data were corrected for the magnetic form factor of Yb^{3+} and Er^{3+} for each energy channel and fixed detector angle, after which several detectors have been grouped together in order to improve statistics. We present further the results in the form of the scattering function $S(Q,\omega)$ versus energy transfer and indicate the incident energy employed for each of them.

RESULTS FOR THE Yb COMPOUNDS

The Hund's rule ground state ($^2F_{7/2}$) of an Yb^{3+} ion in a cubic crystal field splits into two doublets (Γ_6 and Γ_7) and one quartet (Γ_8). Transitions between the two doublets are forbidden ($\langle \Gamma_6 | J_z | \Gamma_7 \rangle = 0$), leaving us with only two transitions ($\Gamma_6 \leftrightarrow \Gamma_8$ and $\Gamma_7 \leftrightarrow \Gamma_8$), with the result that at low temperatures only one excitation is observable if the ground state is a doublet and two are observable if the ground state is the Γ_8 quartet.

$YbAuCu_4$

In Fig. 2 we show the IN6 [Fig. 2(a)–2(c)] and HRMECS spectra [Figs. 2(d)–2(f)] for $YbAuCu_4$ for the same temperatures. At a first view the $YbAuCu_4$ spectra appear to contain only a quasielastic and one inelastic line at any temperature, with the linewidths of the latter increasing with rising temperature. However, integration of the spectra obtained on HRMECS suggests that it contains the full cross section of the $^2F_{7/2}$ ground state of Yb^{3+} so that no further excitation outside the covered energy window is expected. We have performed a fit of the data with a quasielastic and one inelastic Lorentzian spectral component from which the resultant quasielastic linewidth as a function of temperature is shown in Fig. 3. A further result from the fits is that the position of the inelastic peak is strongly temperature dependent, i.e., the center moves to lower energies with increasing temperature (see Fig. 4). Such a strong temperature dependence of the inelastic line can only be explained under the assumption that the 15 K spectrum contains only one inelastic excitation, which takes place from the ground state. With increasing temperature a second excitation with slightly lower transition energy arises (from the first excited state to the next higher level) with a progressively increasing spectral weight and thus shifts the total inelastic spectrum towards smaller energy transfers.

We conclude that the ground state is one of the two doublets, Γ_6 or Γ_7, since only one inelastic excitation is observed at $T = 15$ K. We performed a quantitative crystal-field analysis based on the Lea, Leask, and Wolf formalism[9] and obtain crystal-field parameters W and x that fit the IN6 and HRMECS data consistently at each temperature (see lines in Fig. 2). It was assumed the two inelastic lines have the same widths and that only one quasielastic linewidth exists (see Fig. 3). Note that all linewidths are significantly larger than the instrumental resolution. We determined from the intensity ratio of quasielastic to inelastic scattering that the Γ_7 doublet is the ground state and that the Γ_8 quartet is the first excited level. The ratios of the squares of the inelastic and/or quasielastic matrix elements are

$$|\langle \Gamma_6 | J_z | \Gamma_8 \rangle|^2 / |\langle \Gamma_6 | J_z | \Gamma_6 \rangle|^2 = 2.8$$

and

$$|\langle \Gamma_7 | J_z | \Gamma_8 \rangle|^2 / |\langle \Gamma_7 | J_z | \Gamma_7 \rangle|^2 = 1.36 \ .$$

In Fig. 5 the resulting crystal-field scheme is shown. The corresponding crystal-field parameters are

$$W = -0.225 \pm 0.004 \text{ meV and } x = -0.945 \pm 0.005 \ .$$

These parameters fit the $YbAuCu_4$ data at all temperatures. It should be mentioned that we can fit the data reasonably when assuming a Γ_8 ground state and nearly degenerate Γ_7 and Γ_6 levels, but in order to fit the 50 and 100 K spectra we have to allow for a temperature-dependent W parameter (between 15 and 100 K W increases by $\simeq 10\%$).

We mention a peculiarity of the quasielastic spectrum at low temperatures: for $T \leq 10$ K the quasielastic spectrum cannot be fit with a single quasielastic Lorentzian. We obtain better fits if an additional Gaussian is included. The deviation from a purely quasielastic Lorentzian line shape is demonstrated in Fig. 6(a). The low-energy magnetic scattering centered at about 0.25 meV and the tail of the spectrum (from 1.0 to 1.5 meV) cannot be fit

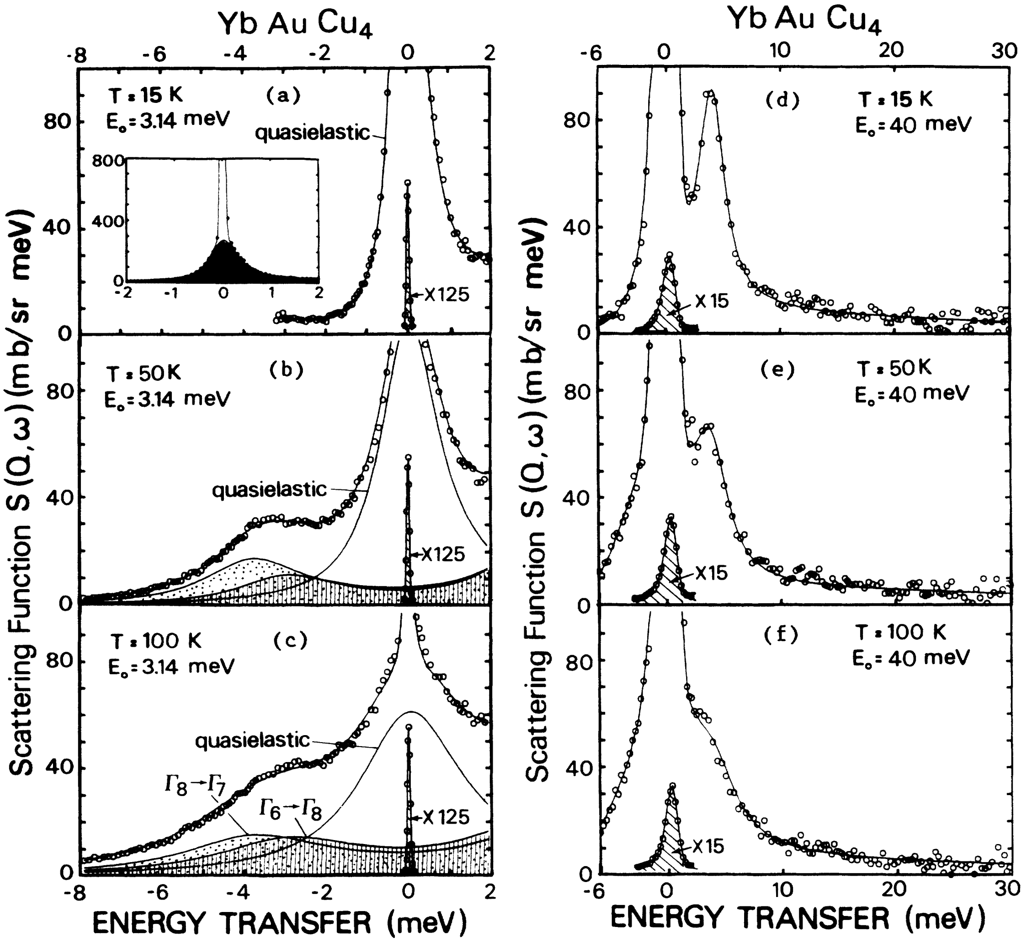

FIG. 2. $YbAuCu_4$ spectra: (a)–(c) energy-gain side of the $E_0 = 3.14$ meV data (IN6) and $17° \leq 2\theta \leq 30°$; the quasielastic scattering is shown as the black area in the inset of (a); (d)–(f) energy-loss side, $E_0 = 40$ meV (HRMECS) and $-7° \leq 2\theta \leq 10°$. The inset lines, marked with the multiplication factors, are due to incoherent elastic scattering. The solid lines are results of quantitative crystal-field analysis. The shaded areas in the IN6 spectra (a)–(c) point out the contribution of the two crystal-field transitions.

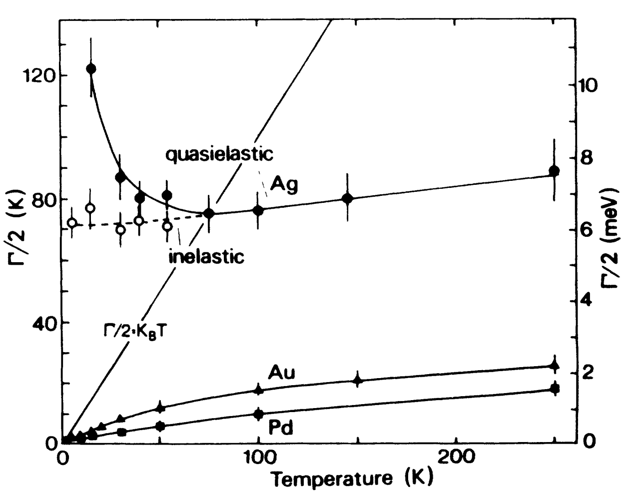

FIG. 3. Linewidth vs temperature: quasielastic Lorentzian width of $YbAuCu_4$ (▲), $YbPdCu_4$ (■), and $YbAgCu_4$ (●). The open circles (○) represent the width of an alternative fit of the $YbAgCu_4$ data below 75 K with an inelastic Lorentzian.

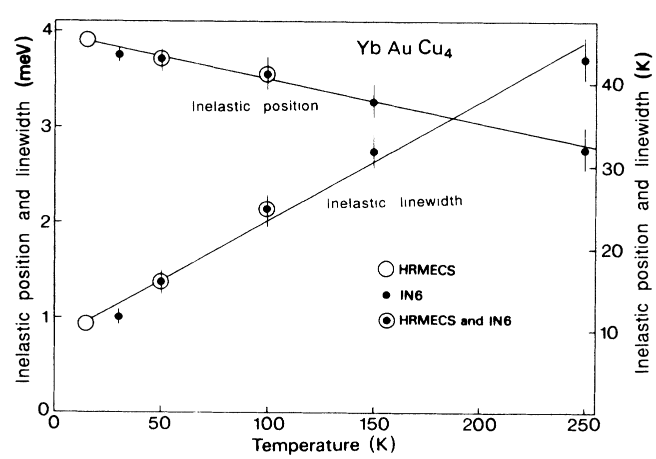

FIG. 4. Temperature dependence of the position and width of the inelastic line, when fitting the $YbAuCu_4$ spectra with one quasielastic and one inelastic Lorentzian.

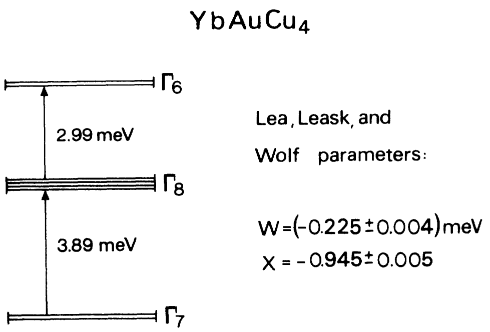

FIG. 5. Crystal-field scheme and crystal-field parameters of YbAuCu$_4$.

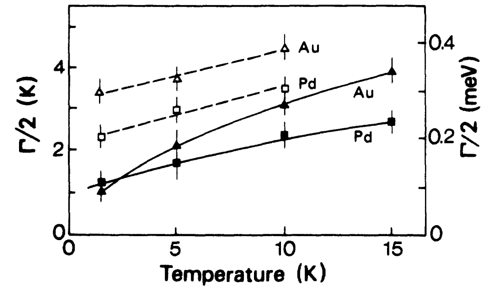

FIG. 7. Quasielastic linewidth of YbXCu$_4$, X=Pd, and Au, below T=15 K. The full symbols represent the Lorentzian width, the open symbols the Gaussian.

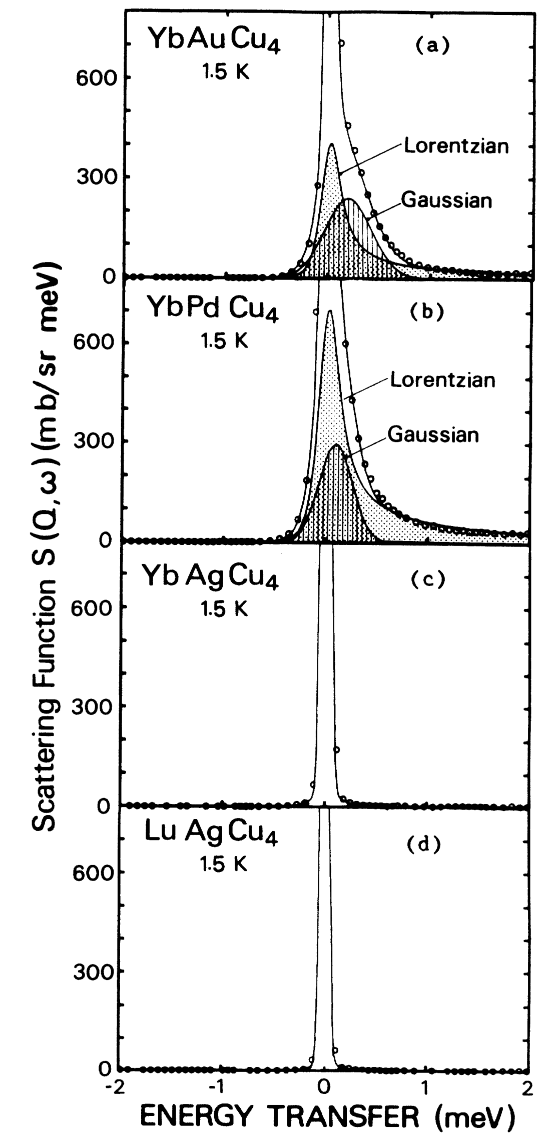

FIG. 6. Spectra of the magnetic YbXCu$_4$ compounds, X=Au, Pd, and Ag, and the nonmagnetic reference sample LuAgCu$_4$ for T=1.5 K and E_0=3.14 meV (IN6).

simultaneosly with one Lorentzian, although the inelastic scattering due to crystal-field splittings is taken into account. With decreasing temperature the Gaussian contribution becomes stronger. For $T=1.5$ K the ratio of the integrated intensities amounts to $\sigma_{\rm Lor}/\sigma_{\rm Gau}\simeq 1.58$. The linewidth of the Gaussian is larger than that of the Lorentzian as shown in Fig. 7 (triangles).

YbPdCu$_4$

The YbPdCu$_4$ spectra are depicted in Fig. 8 for various temperatures and three different incident energies. A comparison of the YbPdCu$_4$ and the YbAuCu$_4$ spectra shows that the quasielastic scattering for the Pd-based sample is narrower, while the inelastic scattering is broader than for YbAuCu$_4$ [for the quasielastic scattering compare the insets in of Figs. 8(a) and 2(a)]. In Table II quasielastic and inelastic linewidths are listed for similar temperatures for the two compounds.

The quasielastic and inelastic spectral weights of YbPdCu$_4$ are comparable with the respective weights of YbAuCu$_4$ so that the same crystal-field level scheme is assumed, although the smaller quasielastic but larger inelastic linewidth in YbPdCu$_4$ seems to be a contradiction. However, earlier we have pointed out that the YbPdCu$_4$ sample exhibits a non-negligible amount of impurity phases. Since each Yb^{3+} ion experiences a crystal-field splitting corresponding to its respective lattice environment, the spectra may be interpreted as the superposition of different crystal-field splittings, corresponding to the different impurity phases. Therefore, it was impossible to perform a quantitative crystal-field analysis for this sample. Instead, the spectra are fitted with a simple quasielastic and inelastic Lorentzian.

The quasielastic linewidth as function of temperature is given in Fig. 3 (squares). For $T\leq 10$ K the quasielastic line shape deviates from a Lorentzian [see Fig. 6(b)], so that an additional Gaussian is included in the fit, as before in YbAuCu$_4$. The Gaussian is broader than the Lorentzian (see Fig. 7, squares) and at T=1.5 K the ratio of the integrated intensities is $\sigma_{\rm Lor}/\sigma_{\rm Gau}\simeq 2.3$.

YbAgCu$_4$

The magnetic excitation spectrum for YbAgCu$_4$ (Fig. 9) is markedly different from the spectra of YbAuCu$_4$ and

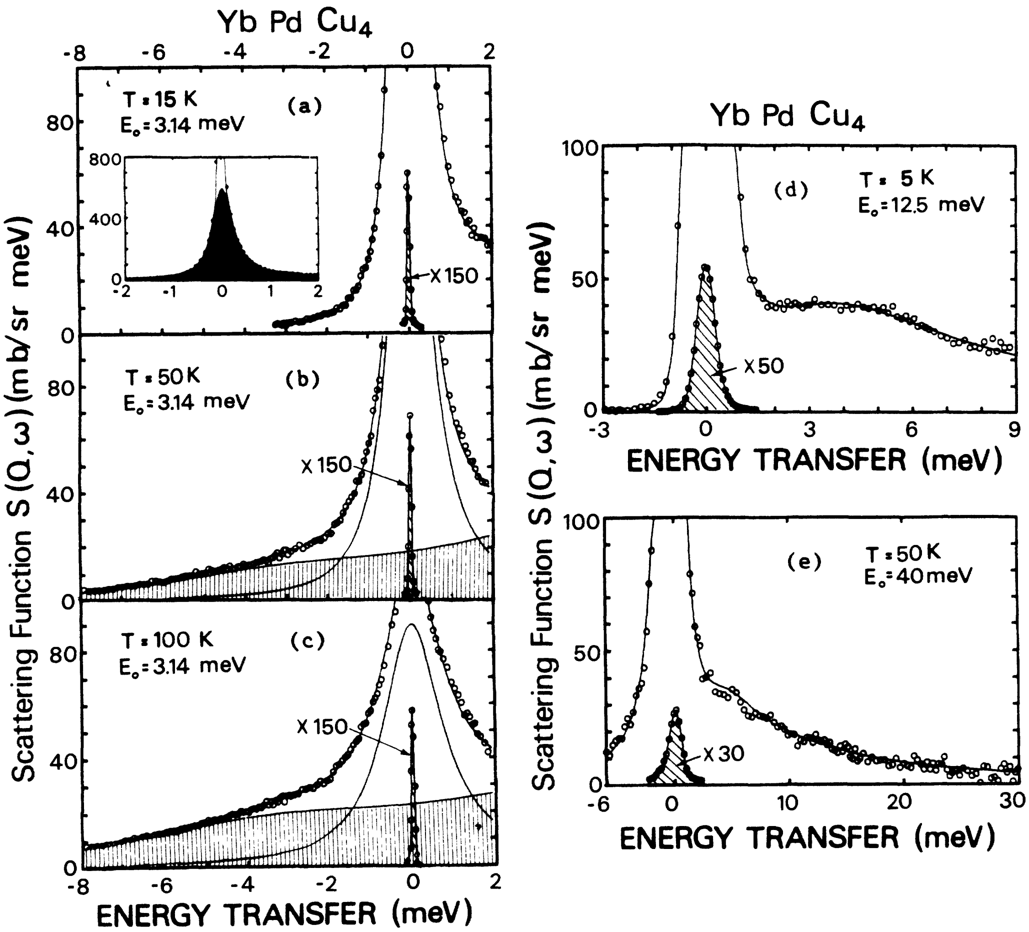

FIG. 8. $YbPdCu_4$ spectra: (a)–(c) energy-gain spectra with $E_0=3.14$ meV (IN6); the quasielastic scattering is shown as the black area in the inset of (a); (d) energy-loss spectra with $E_0=12.5$ meV (IN4) and (e) $E_0=50$ meV (IN4). The inset lines, marked with the multiplication factors, are due to incoherent elastic scattering. The solid lines are fits with one quasielastic and one inelastic Lorentzian. The vertically hatched areas in the IN6 spectra represent the inelastic contribution.

$YbPdCu_4$ as expected since its bulk susceptibility is highly anomalous and very different from those of the other two. The differences in the dynamic susceptibility become most obvious when we compare the IN6 data at $T=1.5$ K (see Fig. 6): $YbAgCu_4$ shows only negligible scattering at small energy transfers in contrast to the Au- and Pd-based samples. The small amount of scattering from $YbAgCu_4$ in this energy range is comparable with that from the nonmagnetic reference $LuAgCu_4$.

For $T>75$ K the $YbAgCu_4$ data can be fit with only one quasielastic Lorentzian that contains the total Yb^{3+} ($^2F_{7/2}$) magnetic cross section within an uncertainty of 10%. The quasielastic linewidth is about a factor 4 larger than for the two other samples (see full circles in Fig. 3). With decreasing temperature ($T\leq 75$ K) the quality of a quasielastic fit becomes progressively worse, as demonstrated in Figs. 9(d)–9(g); the dashed lines in the spectra (obtained with $E_0=40$ meV) represent the best quasielastic fit possible. Furthermore, the obtained quasielastic linewidth $\Gamma/2$ shows a rather unusual temperature dependence below 75 K; for $T<75$ K $\Gamma/2$ increases with continuously decreasing temperature (see full circles in Fig. 3).

Alternatively, if we attempt to represent the spectral response for $T<75$ K by using a single inelastic Lorentzian, we obtain good fits with essentially the same parameters for HRMECS and IN6 data (see solid lines in Figs. 9(d)–9(g)). In addition, the linewidth of the inelastic Lorentzian yields a more sensible temperature dependence, namely, below 75 K the inelastic linewidth $\Gamma_i/2$ joins continuously with the quasielastic width (for $T>75$

TABLE II. Quasielastic $\Gamma/2$ and inelastic $\Gamma_i/2$ linewidth half width at half maximum (HWHM) of $YbAuCu_4$ and $YbPdCu_4$. The respective temperatures are given in parenthesis.

X	$\Gamma/2$ (meV)	$\Gamma_i/2$ (meV)
Au	0.35 ($T=15$ K)	0.93 ($T=15$ K)
Pd	0.23 ($T=5$ K)	3.32 ($T=5$ K)

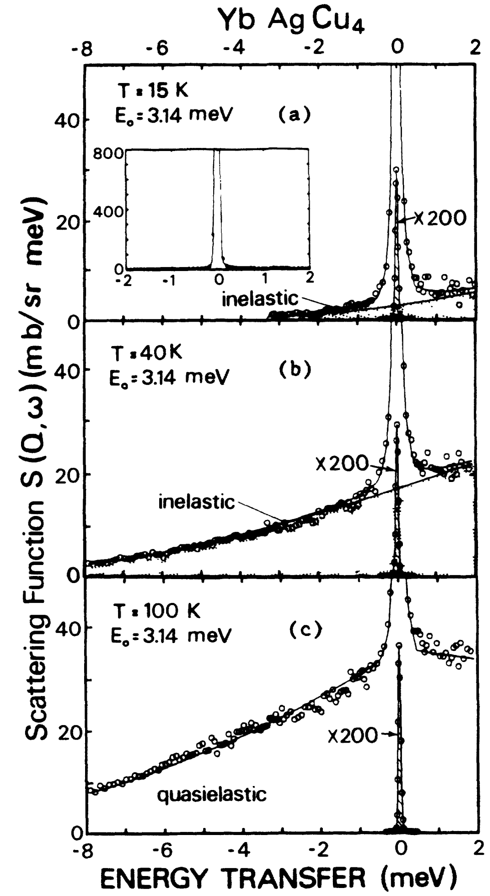

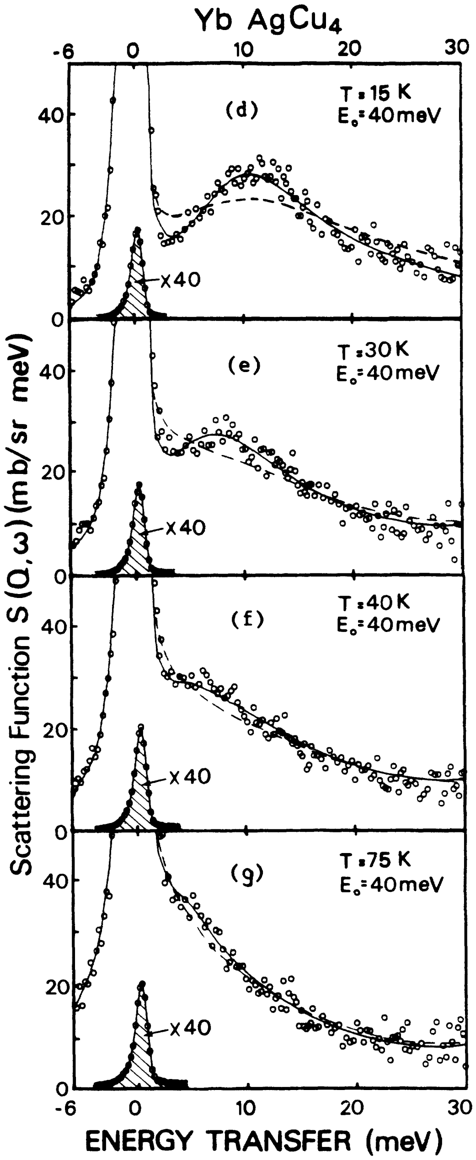

FIG. 9. $YbAgCu_4$ spectra: (a)–(c) energy-gain with $E_0 = 3.14$ meV (IN6); the inset in (a) demonstrates the small amount of low-energy scattering in comparison to Figs. 1(a) and 8(a); (d)–(g) energy-loss spectra with $E_0 = 40$ meV (HRMECS). The inset lines, marked with the multiplication factors, are due to incoherent elastic scattering. The solid lines in the spectra (d)–(g) represent an inelastic Lorentzian fit, the dashed lines a quasielastic fit.

K) and $\Gamma_i/2$ reaches a finite value for $\Gamma \rightarrow 0$ K. For $T = 55$ K the inelastic line is centered at $\hbar\omega_i = 3.0$ meV. With decreasing temperature its position moves towards larger energy transfers such that its energy and width are comparable at $T = 15$ K. The static susceptibility $\chi(Q)/|F(Q)|^2$ calculated in absolute units from the quasielastic ($T \geq 75$ K) and inelastic ($T < 75$ K) Lorentzian fits agree very well with the static bulk susceptibility at all temperatures (Fig. 10).

RESULTS FOR THE Er COMPOUNDS

The Hund's rule ground state of Er^{3+} ($J = \frac{15}{2}$) with cubic-site symmetry splits into two doublets (Γ_6 and Γ_7) and three quartets ($\Gamma_8^{(1)}$, $\Gamma_8^{(2)}$, and $\Gamma_8^{(3)}$). All transitions are allowed except $\Gamma_6 \leftrightarrow \Gamma_7$ so that at most nine transitions are observable. In Fig. 11 the $ErXCu_4$ spectra (X= Ag, Au, and Pd) are shown for two different incident energies. The data obtained with 17 meV incident energy yield information up to 15 meV energy transfer. Additional measurements carried out with $E_0 = 67$ meV at $T = 50$ and 100 K verified that no excitations of observable intensity exist in the energy range from 15 to $\simeq 50$ meV.

It is often useful in determination of crystal-field schemes to identify the excitations from the ground state. For that purpose, measurements at temperatures small compared to the crystal-field splitings between the lowest

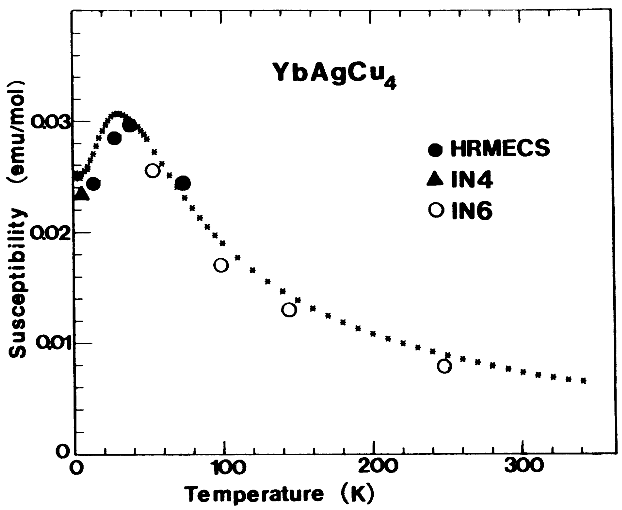

FIG. 10. Bulk susceptibility of $YbAgCu_4$: ($*$) spectrometer values; (○, ●, and ▲) neutron values, determined via integration over the $\chi''(\omega)$. The values below 75 K are determined from an inelastic fit, the values for $T \geq 75$ K from a quasielastic one.

two levels are necessary. Although we measured down to very low temperatures (1.5 K), we were not able to determine the ground-state excitations, since the onset of magnetic order, which lifts the degeneracies, further prevented a proper analysis of the $T=1.5$, 3, and 5 K data. In the extreme case, i.e., in the presence of a high internal magnetic field, the ground state would be the $m_J=-\frac{15}{2}$ Zeeman state. At temperatures reasonably high above the ordering transition, i.e., at $T=15$, 20, or 30 K (see Fig. 11), all the crystal-field levels are already populated so that transitions from the ground state are not identifiable. Furthermore, due to the internal molecular field the broadening of the intrinsic linewidths in these concentrated compounds (in contrast to diluted systems) prevents the peaks from being well resolved. As a result we could not determine crystal-field schemes by fitting the data. The solid lines in Fig. 11 indicate fits with one quasielastic and several inelastic Lorentzians carried out to represent the data. For $T=15$ K the quasielastic linewidths are $\Gamma/2=0.11$, 0.13, and 0.05 meV for $X=$Ag, Au, and Pd, respectively.

As described later, however, we could fit the data for $ErAuCu_4$ to a crystal-field scheme by scaling the crystal-

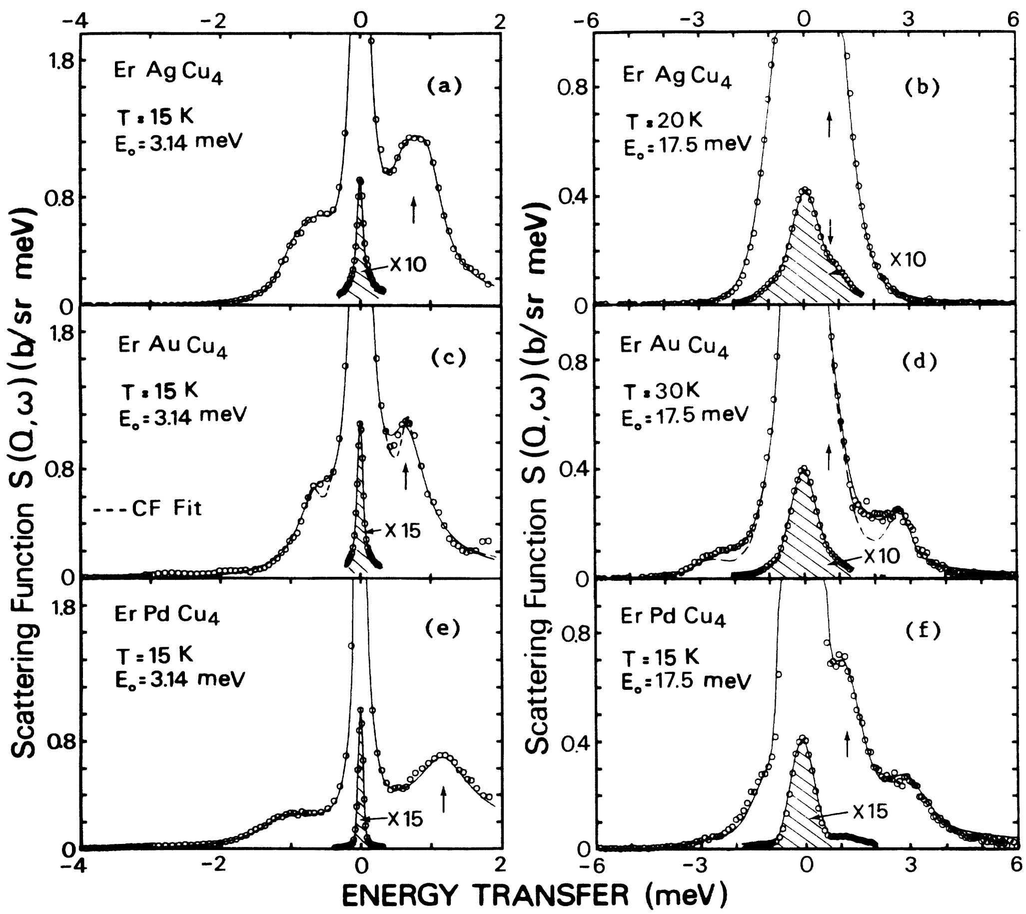

FIG. 11. IN4 (b), (d), and (f) and IN6 (a), (c), and (e) spectra of $ErXCu_4$, $X=$Ag, Au, and Pd with $E_0=17$ and 3.14 meV, respectively. The arrows mark identical energy transfers in the IN4 and IN6 spectra. The solid lines represent fits with the quasielastic and inelastic lines. The dashed line in the $ErAuCu_4$ spectra results from the calculated crystal-field parameters.

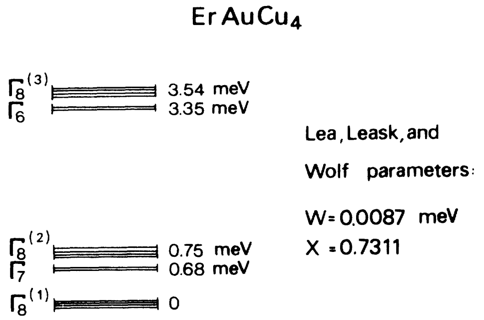

FIG. 12. Crystal-field scheme and crystal-field parameters of $ErAuCu_4$, calculated from the crystal-field parameters of $YbAuCu_4$.

field parameters of Yb^{3+} in $YbAuCu_4$ to Er^{3+} in $ErAuCu_4$ (see Fig. 12). From the overall results we can make the statement that the total crystal-field splitting decreases in the sequence Pd→Au→Ag within the ErXCu$_4$ series.

ErAuCu$_4$

For diluted systems it has been shown in the past that the crystal-field parameters A_L^m are roughly the same for Yb^{3+} and Er^{3+}.[10,11] This allows us to calculate the Lea, Leask, and Wolf parameters W and x for Er^{3+} in $ErAuCu_4$ from the corresponding values of Yb^{3+} in $YbAuCu_4$ assuming that the crystal-field parameters A_l^m are identical for Yb^{3+} and Er^{3+}. The A_l^m can be expressed in terms of W and x by

$$A_4^0=[\beta_J F(4)\langle r^4\rangle]^{-1}xW$$

and

$$A_6^0=[\gamma_J F(6)\langle r^6\rangle]^{-1}(1-|x|)W \ .$$

The Stevens factors β_J and γ_J, the expectation values $\langle r^l\rangle$ and the factors $F(l)$ are listed in the literature (see, for example, in Ref. 7).

Using the values of x and W obtained for $YbAuCu_4$ for the Γ_7 ground state (see Fig. 5), the listed values for β_J, γ_J, $\langle r^l\rangle$, and $F(l)$, and assuming identical A_l^m for Er^{3+} and Yb^{3+} in the compounds RAuCu$_4$ (R=Yb and Er), we obtain

$$W=0.0087 \text{ meV and } x=0.7311 \ .$$

The dashed line in the spectra for $ErAuCu_4$ [Figs. 11(c)–11(d)] corresponds to a crystal-field fit with the values of x and W given earlier. This fit is quite remarkable, although not perfect, considering the dramatic variation of the transition-matrix elements between the various crystal-field levels of Er^{3+} with varying x.[12] On the other hand, a fit with crystal-field parameters calculated from W and x values belonging to a Γ_8 ground state in $YbAuCu_4$ yields neither correct energy positions nor intensity ratios. Therefore, the fairly good agreement of the crystal-field fit to the $ErAuCu_4$ spectra resulting from the Γ_7 ground-state parameters of $YbAuCu_4$ asserts the correctness of the crystal-field scheme of $YbAuCu_4$ shown in Fig. 5.

DISCUSSION

YbAuCu$_4$ and YbPdCu$_4$

For $T=15$ K the quasielastic linewidths of $YbAuCu_4$ and $YbPdCu_4$ are about 4 times larger than those of the corresponding Er compounds. Furthermore, the width of the quasielastic line at T=250 K, the T dependence of $\Gamma/2$ (roughly a $T^{1/2}$ power law), and the existence of crystal-field excitations compare with the neutron scattering response of other concentrated Kondo systems such as $CeAl_2$,[13] CeB_6,[13] $CeInCu_2$,[14] $CePd_2Si_2$,[6] etc., which order magnetically. The Gaussian contribution to the quasielastic scattering in these two samples for $T<10$ K is understood as a precursor of the magnetic order taking place below 1 K.

YbAgCu$_4$

For $T=15$ K the magnetic spectral width of $YbAgCu_4$ is about 80 times broader than the quasielastic linewidth for $ErAuCu_4$. At higher temperatures (T=250 K) the quasielastic line of width $\Gamma/2\simeq 8$ meV is a factor of 4 broader than in $YbAuCu_4$ and $YbPdCu_4$. Hence, we conclude, in agreement with bulk measurements of Rossel *et al.*,[1] that $YbAgCu_4$ is the compound with the most unstable $4f$ shell in the series investigated.

We already pointed out that fits with only one quasielastic line yield neither a satisfactory quality of fit nor a sensible temperature dependence of the linewidth for $T<75$ K, whereas we found that an inelastic Lorentzian describes the data better. The phenomenon of a quasielastic spectrum becoming inelastic below a certain temperature has been observed in several Ce (Refs. 3–6) and Yb compounds,[7,8] however, the exact interpretation of such a spectral response is still a subject of discussion. The compounds which show this type of behavior have in common an anomalous temperature dependence of the static susceptibility, i.e., χ_{stat} is Pauli-like at low T, goes through a maximum, and becomes Curie-Weiss-like at high temperatures. In the following, the results for $YbAgCu_4$ data are discussed in terms of the usual crystal-field interpretation as well as with reference to models, describing the dynamic susceptibility of materials with unstable $4f$ moments.

Crystal field

The possibility that $YbAgCu_4$ spectra represent excitations within the crystal-field-split Hund's-rule ground state of Yb^{3+} cannot be excluded. For example, the spectrum for T=15 K and E_0=40 meV can be fit with a quasielastic and an inelastic line and spectral weights consistent with the crystal-field analysis of the $YbAuCu_4$ data, i.e., if we assume the x parameter to be the same as for $YbAuCu_4$ and fit W, we obtain a crystal-field scheme with a Γ_7 ground state, the Γ_8 quartet 9.3 meV above the ground state, and the Γ_6 7.2 meV above the Γ_8 level. The resulting W parameter is twice as large as for $YbAuCu_4$ ($W=-0.54$ meV and $x=\text{const}=-0.945$). In order to fit the high- [see Fig. 9(d)] and low-energy range [see Fig. 9(a)] simultaneously a quasielastic linewidth of $\Gamma/2 \geq 8$ meV has to be assumed. The inelastic linewidths are comparable with the quasielastic width.

Within such a crystal-field interpretation the temperature dependence of the $YbAgCu_4$ spectra can be understood in the following way: below 75 K the quasielastic linewidth is comparable with the crystal-field splitting, and the excitation from the ground state to the first excited level can be resolved. However, above 75 K the quasielastic line becomes broader than the crystal-field splitting so that the quasielastic line smears out the inelastic scattering. In addition, the transition from the first excited to the highest crystal-field level becomes stronger with increasing temperature. Consequently, no discrete peaks are observed. This may explain why the spectrum can be fit to a pure quasielastic distribution at high temperatures. For this analysis a knowledge of the crystal-field parameters of $ErAgCu_4$ would be quite useful since we should expect a fit with crystal-field parameters (for Yb^{3+} in $YbXCu_4$) calculated from the ones for Er^{3+} in $ErXCu_4$ (analogously to $YbAuCu_4$ and $ErAuCu_4$) could help to prove or disprove the cyrstal-field interpretation.

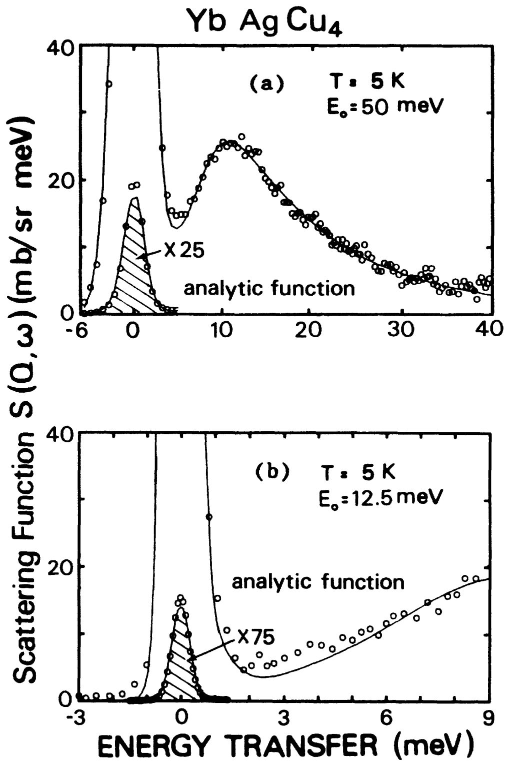

FIG. 13. $YbAgCu_4$ spectra at $T=5$ K with $E_0=50$ and 12.5 meV (IN4). The inset lines are due to elastic incoherent scattering. The spectra are fitted with an analytic function for $\chi''(\omega)$ in the limit $T\rightarrow 0$, given by Kuramoto and Müller-Hartmann (see text). Both spectra are fitted with the same parameters.

Comparison with models of $4f$ compounds having unstable $4f$ configurations

In the following the $YbAgCu_4$ data are discussed in terms of theories describing the magnetic relaxation behavior of $4f$ unstable materials. Several theories predict that the magnetic scattering function, which is quasielastic at high temperatures, becomes inelastic below a certain temperature. These theories are based on the Anderson model in the limit $U\rightarrow\infty$ ($U=4f$-$4f$ Coulomb repulsion). A characteristic temperature T_0 can be determined from the line shape of the dynamic susceptibility $\chi''(\omega)$ for $T\rightarrow 0$ and from the temperature dependence of the energy width of $\chi''(\omega)$.

Bickers *et al.*[15] predict a deviation of the line shape of the magnetic scattering from a quasielastic Lorentzian for $T<T_0$ (T_0=position of the Kondo resonance measured from the Fermi level). First of all, the quasielastic linewidth $\Gamma/2$ decreases with decreasing temperature. When the spectrum is fit to a quasielastic distribution at all temperatures, i.e., even for $T<T_0$, then Γ_2 shows a minimum at $T=T_0$ and increases again with decreasing temperature. The temperature T_0 of the minimum of the quasielastic linewidth of $YbAgCu_4$ can be considered to represent a characteristic temperature ($T_0 \simeq 75$ K).

Within Schlottmann's model[16] the magnetic scattering is quasielastic at high temperatures and at low temperatures centered around the characteristic energy $h\omega=E_{ex}$, where E_{ex} is the excitation energy of a $4f$ electron into the conduction band. We obtain $E_{ex}/k_B=T_0=103$ K for $YbAgCu_4$, if the position of the inelastic peak at $T=5$ K is identified with the characteristic energy. The spin-relaxation rate is given by the width of the spectrum, and from Schlottmann's calculations a nearly temperature-independent relaxation rate is expected. This agrees with the $YbAgCu_4$ data quite well: the relaxation rate of $YbAgCu_4$ is represented by the quasielastic linewidth $\Gamma/2$ at high temperatures and by the inelastic one $\Gamma_i/2$ below 75 K. $\Gamma/2$ passes over smoothly into $\Gamma_i/2$ and the total tempeature dependence is very weak (see Fig. 3, full

TABLE III. Characteristic temperatures of $YbAgCu_4$ determined from the neutron scattering data, the bulk susceptibility $\chi_{\text{bulk}}(T=0)$, and the linear coefficient of the specific heat.

	Characteristic temperature
Minimum of $\Gamma/2$ vs temperature, Bickers *et al* (Ref. 15) (neutron data, forced quasielastic fit)	$T_0=75$ K
Position of inelastic hump, Schlottmann (Ref. 16) (neutron data at $T=5$ K)	$E_{ex}/k_B=103$ K
Analytic function of $\chi''(\omega)$ Kuramoto *et al* (Ref. 17) (neutron data at $T=5$ K)	$E_{ex}/k_B=96$ K
$\chi_{\text{bulk}}(T=0)$, Ramakrishnan and Sur (Ref. 18)	$E_{ex}/k_B=92$ K
Linear coefficient γ of C_v, Ramakrishnan and Sur (Ref. 18)	$E_{ex}/k_B=112$ K

circles for $T > 75$ K and open circles for $T < 75$ K).

Kuramoto and Müller-Hartmann[17] give an analytic function for $\chi''(\omega)$ at $T=0$, which we have fit to the $YbAgCu_4$ data at $T=5$ K. The variables in this function are the ratio of the $4f$ occupancy to the degeneracy of the ground state (n_f/N) and the characteristic energy parameter E_{ex} (position of the normalized $4f$ level relative to the Fermi level). In Fig. 13(a) the 50 meV spectrum is shown for $T=5$ K, fit with the analytic function. The low-energy part of the spectrum (<6 meV) was excluded from the fitting range, since, as the authors of Ref. 13 point out, their analytic function underestimates the real spectrum by as much as 20% for $\hbar\omega \rightarrow 0$ [compare the 12 meV spectrum in the bottom part of Fig. 13(b)]. The resulting fit parameters are

$$\alpha = 0.147\ (\pm 15\%),\quad E_{ex}/k_B = 96\ \mathrm{K}\ (\pm 8\%)\ .$$

From the value of α assuming $4f$ occupancy $n_f=1$ we obtain a degeneracy N of the ground state of

$$N = 6.8\ (\pm 1.0)\ .$$

Within the uncertainty, this value of N is consistent with the full degeneracy of $2J+1=8$ of an Yb^{3+} ion.

Ramakrishnan and Sur[18] have calculated thermodynamic properties of intermediate-valent materials and expressed the bulk susceptibility χ_{bulk} and the linear coefficient of the specific heat for $T=0$ in terms of an energy parameter E_{ex} (E_{ex} = energy difference of the renormalized $4f$ levels).

$$\chi_{bulk}(T=0) = \tfrac{1}{3}\mu_{eff}^2 n_f / E_{ex}\ ,$$

$$\gamma = \tfrac{2}{3}\pi n_f k_B / E_{ex}\ ,$$

μ_{eff} being the effective magnetic moment. We have calculated E_{ex} from the susceptibility (Fig. 10) and the value of γ given in Ref. 1 [$\chi_{bulk}(T=0)=0.025$ emu/mol and $\gamma=245$ mJ/mol K^2] and obtain $E_{ex}/k_B=92$ and 112 K, respectively.

The characteristic temperatures determined from neutron scattering, the bulk susceptibility and the linear coefficient of the specific heat are listed in Table III. The relatively good agreement amongst the variously determined values for the characteristic temperatures (energies) suggests that the observed magnetic response of $YbAgCu_4$ could be understood in terms of an intermediate-valent (single-ion model).

CONCLUSION

The quasielastic linewidth of the magnetically ordering compounds $YbAuCu_4$ and $YbPdCu_4$ follow roughly a $T^{1/2}$ power law with a width of about 2 meV at $T=250$ K, and both compounds show crystal-field excitations, which are broadened because of interactions between $4f$ and conduction electrons. For $YbAuCu_4$ the crystal-field scheme and crystal-field parameters have been determined (Γ_7 ground state), asserted by the crystal-field fit of the $ErAuCu_4$ spectra. Because of some impurity phases no quantitative crystal-field analysis could be performed for $YbPdCu_4$.

The magnetic spectral width of the magnetically nonordering compound $YbAgCu_4$ is almost temperature independent (8 meV), however, the spectral shape changes from quasielastic at high temperatures ($T>75$ K) to inelastic below $\simeq 75$ K such that at $T=15$ K the width and energy of the inelastic peak are comparable. The magnetic response of $YbAgCu_4$ has been discussed in terms of a crystal-field interpretation as well as in terms of theories, based on the Anderson model, which calculate $\chi''(\omega)$ for materials with an unstable $4f$ shell. These models yield, in agreement with the specific heat and bulk susceptibility, a characteristic temperature of $E_{ex}/k_B \simeq 100$ K.

ACKNOWLEDGMENTS

Work at Los Alamos was performed under the auspices of the U.S. Department of Energy, Office of Basic Energy Science, Division of Material Science. One of us (A.S.) was supported by the Sonderforschungsbereich 125 and the Bundes Ministerium für Forschung und Technologie of the Federal Republic of Germany.

[1]C. Rossel, K. N. Yang, M. B. Maple, Z. Fisk, E. Zirngiebl, and J. D. Thompson, Phys. Rev. B **35**, 1914 (1987).

[2]P. A. Lee, T. M. Rice, J. W. Serene, L. G. Sham, and J. W. Wilkins, Comments Cond. Mater. Phys. **12**, 99 (1986).

[3]A. P. Murani, Phys. Rev. B **28**, 2308 (1983); J. Phys. C **33**, 6359 (1983).

[4]R. M. Galera, D. Givord, J. Pierre, A. P. Murani, C. Vettier, and K. R. A. Ziebeck, J. Magn. Magn. Mater. **63&64**, 594 (1985).

[5]A. P. Murani, W. C. M. Mattens, F. R. de Boer, and G. H. Lander, Phys. Rev. B **31**, 52 (1985).

[6]C.-K. Loong, B. H. Grier, S. M. Shapiro, J. M. Lawrence, R. D. Parks, and S. K. Sinha, Phys. Rev. B **35**, 3092 (1987).

[7]A. P. Murani, Phys. Rev. Lett. **54**, 1444 (1985); Phys. Rev. B **36**, 5705 (1987).

[8]A. Severing, E. Holland-Moritz, and B. Frick, Phys. Rev. B **39**, 4164 (1989).

[9]K. R. Lea, M. J. M. Leask, and W. P. Wolf, J. Phys. Chem. Solids **23**, 1381 (1982).

[10]U. Walter and E. Holland-Moritz, Z. Phys. B **45**, 107 (1981).

[11]B. Frick and M. Loewenhaupt, Z. Phys. B **63**, 213 (1981); **63**, 231 (1981).

[12]R. J. Birgenau, J. Phys. Chem. Solids **33**, 59 (1972).

[13]S. Horn, F. Steglich, M. Loewenhaupt, and E. Holland-Moritz, Physica **107B**, 103 (1981).

[14]R. Lahiouel, Ph.D. thesis, L'Universite Scientifique Technologique et Medicale de Grenoble, 1987.

[15]N. E. Bickers, D. L. Cox, and J. W. Wilkins, Phys. Rev. B **36**, 2036 (1987).

[16]P. Schlottmann, Phys. Rev. B **25**, 2371 (1982); **29**, 4468 (1984).

[17]Y. Kuramoto and E. Müller-Hartmann, J. Magn. Magn. Mater. **52**, 122 (1985).

[18]T. V. Ramakrishnan and K. Sur, Phys. Rev. B **26**, 1798 (1982).

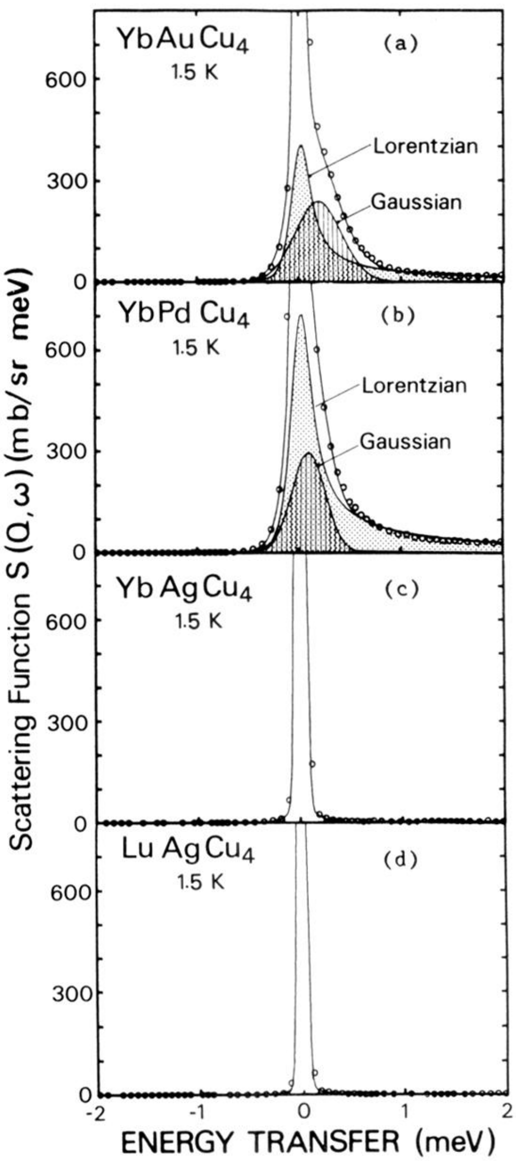

FIG. 6. Spectra of the magnetic YbXCu$_4$ compounds, X=Au, Pd, and Ag, and the nonmagnetic reference sample LuAgCu$_4$ for T=1.5 K and E_0=3.14 meV (IN6).

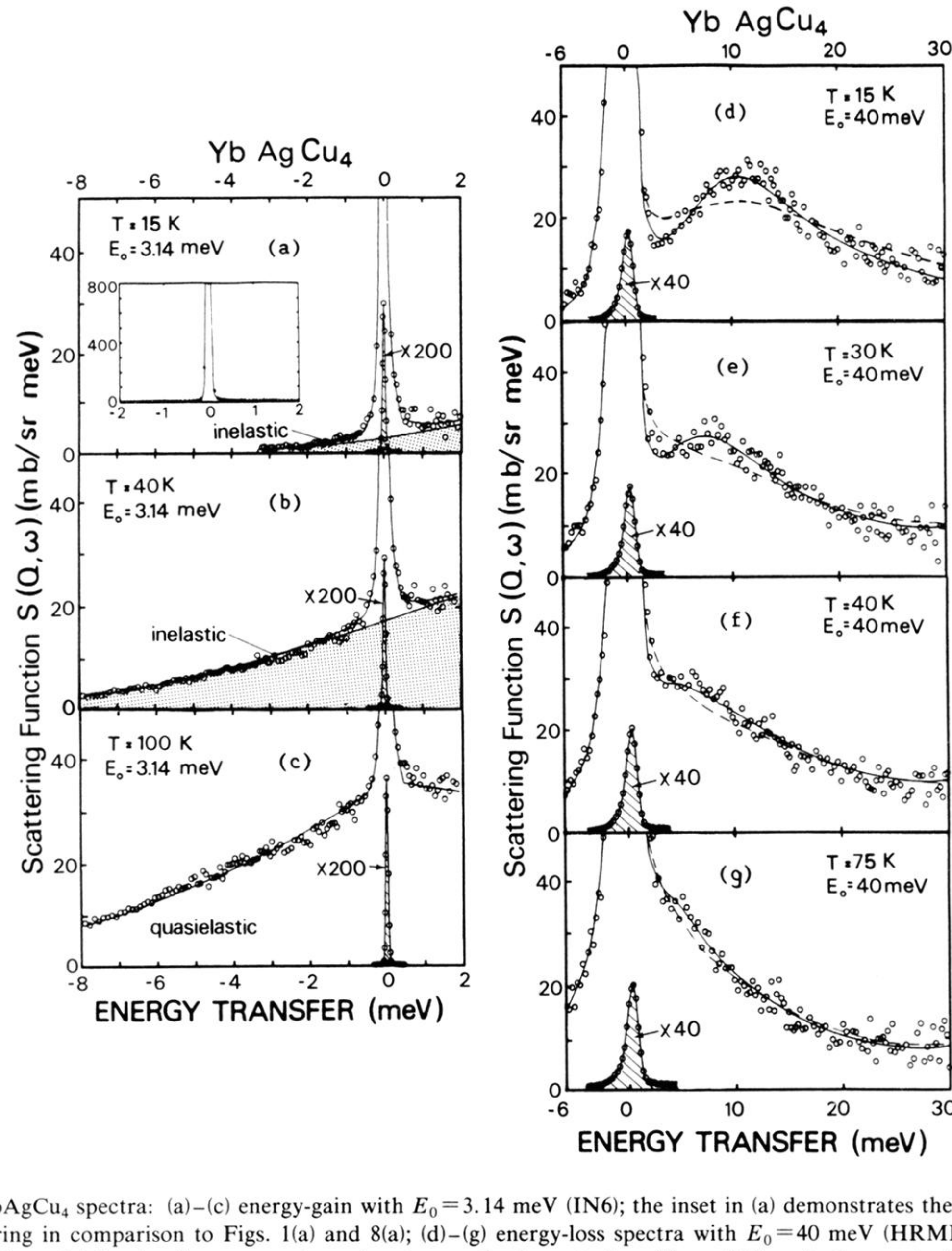

FIG. 9. $YbAgCu_4$ spectra: (a)–(c) energy-gain with $E_0=3.14$ meV (IN6); the inset in (a) demonstrates the small amount of low-energy scattering in comparison to Figs. 1(a) and 8(a); (d)–(g) energy-loss spectra with $E_0=40$ meV (HRMECS). The inset lines, marked with the multiplication factors, are due to incoherent elastic scattering. The solid lines in the spectra (d)–(g) represent an inelastic Lorentzian fit, the dashed lines a quasielastic fit.